NAA-SR-3170
COPY

DIFFUSION OF BERYLLIUM IN BERYLLIUM OXIDE

AEC Research and Development Report

ATOMICS INTERNATIONAL
A DIVISION OF NORTH AMERICAN AVIATION, INC.

NAA-SR-3170
METALLURGY AND CERAMICS
22 PAGES

DIFFUSION OF BERYLLIUM IN BERYLLIUM OXIDE

BY
STANLEY B. AUSTERMAN

ATOMICS INTERNATIONAL
A DIVISION OF NORTH AMERICAN AVIATION, INC.
P.O. BOX 309 CANOGA PARK, CALIFORNIA

CONTRACT: AT(11-1)-GEN-8
ISSUED: DECEMBER 15, 1958

DISTRIBUTION

This report has been distributed according to the category "Metallurgy and Ceramics" as given in "Standard Distribution Lists for Unclassified Scientific and Technical Reports" TID-4500 (14th Ed.), October 1, 1958. A total of 600 copies was printed.

CONTENTS

		Page No.
	Abstract.	4
I.	Introduction	5
II.	Experimental Procedure	5
III.	Data and Analysis	11
IV.	Discussion	18
	A. Alternate Diffusion Processes.	18
	B. Effect of Molybdenum Impurity	18
V.	Summary	21
	References	22

TABLES

I.	Spectrographic Analyses	6
II.	Diffusion Data	16

FIGURES

1.	Photomicrograph of an ET1 Sample, Polished and Etched, after 2000°C Preliminary Anneal	8
2.	Cut-away Section of Plastic Mount and Holder for Positioning Sample under Scintillation Counter	10
3.	Be^7 Distribution after 1570°C Anneal	13
4.	Be^7 Distribution after 1676°C Anneal	13
5.	Be^7 Distribution after 1723°C Anneal	14
6.	Be^7 Distribution after 1777°C Anneal	14
7.	Be^7 Distribution after 1824°C Anneal	15
8.	Be^7 Distribution after 1878°C Anneal	15
9.	Be^7 Distribution after 1934°C Anneal	17
10.	Log D vs 1/T for Diffusion of Be^7 in BeO	19

ABSTRACT

The self-diffusion of Be in polycrystalline BeO was determined with radioactive Be^7 at temperatures between 1570° and 1934°C. Following diffusion anneal, the samples were sectioned by grinding, and the one-dimensional diffusion-penetration of Be^7 was determined by counting procedures. The data can be fitted by two straight lines on a log D vs 1/T graph. The temperature region 1570° to 1730°C was fitted by

$$D = 5.56 \times 10^3 \exp(-111{,}600/RT).$$

The region 1730° to 1934°C was fitted by

$$D = 6.14 \times 10^{-2} \exp(-66{,}100/RT).$$

There was no evidence of grain-boundary diffusion.

I. INTRODUCTION

The process of self-diffusion is important to many high-temperature phenomena, including grain-growth, sintering, solid-state chemical reactions, and plastic deformation.[1,2,3] For assistance in interpreting the role of self-diffusion in these phenomena for beryllium oxide, the present experiment was undertaken to determine the magnitude and temperature dependence of diffusion of the beryllium ion in BeO.

II. EXPERIMENTAL PROCEDURE

The experiments were performed by tracer techniques, using the radioactive tracer Be^7. The tracer was applied to a flat surface on each sample so that one-dimensional diffusion would occur during subsequent anneal. The tracer distribution in each annealed body was then determined by sectioning, and counting with a shielded scintillation counter.

Beryllium of mass seven has convenient properties for use as a tracer isotope. Its mode of decay is by K-capture, with about 11 percent of the disintegrations accompanied by emission of a 0.48 Mev gamma.[4,5] This disintegration is unaccompanied by other radiation; and the daughter product, lithium-seven, is the common nonradioactive lithium isotope. As a result, the counting procedure can be quite simple. Also, the gamma energy, 0.48 Mev, is sufficiently high so that absorption in the BeO is not significant to the depths measured in this experiment. The isotope, procured as Be^7Cl_2 in HCl from Nuclear Science and Engineering Corporation, has a reported radiopurity of > 99 percent. Confirmation of the half-life of the isotope, 54.5 days for Be^7, verified its identity.

In the absence of single crystals it is necessary to use polycrystalline forms of BeO. The sample material chosen as having the most favorable combination of large grain size, high density, and uniform chemical purity that could be readily obtained at the time was a rod, 0.5 inch in diameter by 5 inches, made by National Beryllia Corporation. This rod was made by slip-casting and firing in a gas-fired furnace to a density of 2.735 gm/cm^3, 90.4 percent of theoretical density. Two independent analyses for impurities were obtained and are shown in Table I, stated in weight percent of the oxide of the reported metal impurities.

TABLE I

SPECTROGRAPHIC ANALYSES

Element	Analysis No. 1 (wt %)	Analysis No. 2 (wt %)
Si	-	0.25
Al	0.5	0.25
Fe	-	0.02
Ca	0.01	0.02
Mg	0.05	0.08
All others reported	0.01	0.01

The following steps were performed to prepare the samples for diffusion-annealing.

a) The rod was cut into sample sections of 1/2 inch in diameter by 1/4 inch thick.

b) Samples free of flaws (cracks or exposed gas pores) were ground to a flat surface on SiC abrasive paper.

c) These samples were then given a preliminary anneal at 2000°C for two hours in an argon atmosphere. They were enclosed during heating in a molybdenum muffle within a tantalum resistance furnace described elsewhere.[6] The purpose of this anneal was to remove any surface damage caused by the previous grinding, and to allow any recrystallization or grain growth which might otherwise occur during the diffusion anneal and thereby complicate interpretation. Comparison of the microstructure before and after this preliminary anneal demonstrated a striking difference in grain size and shape and showed that the anneal was necessary.

d) The Be^7 was deposited simultaneously onto the plane surface of each of a number of BeO samples by evaporating the Be^7Cl_2 from a tungsten filament electrically heated in vacuo.

e) To ensure conversion of the Be^7 to the oxide form, the samples were first exposed to $NH_4(OH)$ vapor to form $Be(OH)_2$, then were heated to about 800°C in air in an alumina crucible to drive off H_2O and leave behind BeO.

The microstructure of a typical sample immediately following the 2000°C preliminary anneal is shown in Figure 1. There was no evident change in microstructure due to subsequent diffusion-anneal in any of the samples examined. The grain-size, as it appears in Figure 1, is from about 80 to 100μ . The microstructure also shows closed pores with no interconnections that might serve as special diffusion paths. The average density of the samples, determined after diffusion analysis, was 92.4 percent of theoretical density, with a total spread of 1.6 percent.

For the diffusion-anneal, the sample was again heated in the molybdenum muffle in an argon atmosphere. The temperature was observed with a Leeds and Northrup optical pyrometer sighting on the outside surface of the muffle in the immediate vicinity of the enclosed sample. This observed temperature was corrected downward by a small amount previously determined to be necessary to give the true sample temperature. Specular reflections and radiation end-losses from the furnace accounted for the temperature differences. The pyrometer and optical train were calibrated together both before and after each anneal, to ensure that no calibration change occurred to cause errors in temperature measurement.

The annealing period in each case was within a few minutes of ten hours. The sample was held about five minutes at 200°C below annealing temperature, then the furnace temperature was raised abruptly to the desired annealing temperature. Upon completion of the annealing period, the furnace temperature was dropped quickly. As a reasonable approximation, it was assumed that the sample's thermal lag during heating was compensated by the lag during cooling.

During diffusion anneal each sample was placed immediately facing an identical sample including the deposition of Be^7. The purpose of this operation was to maintain equilibrium conditions at the sample surface, and to minimize loss of both BeO sample surface and deposited Be^7.

To avoid confusion due to possible surface-diffusion down the sides of the sample or due to Be^7 being initially deposited on the sides, 1/16 inch of material

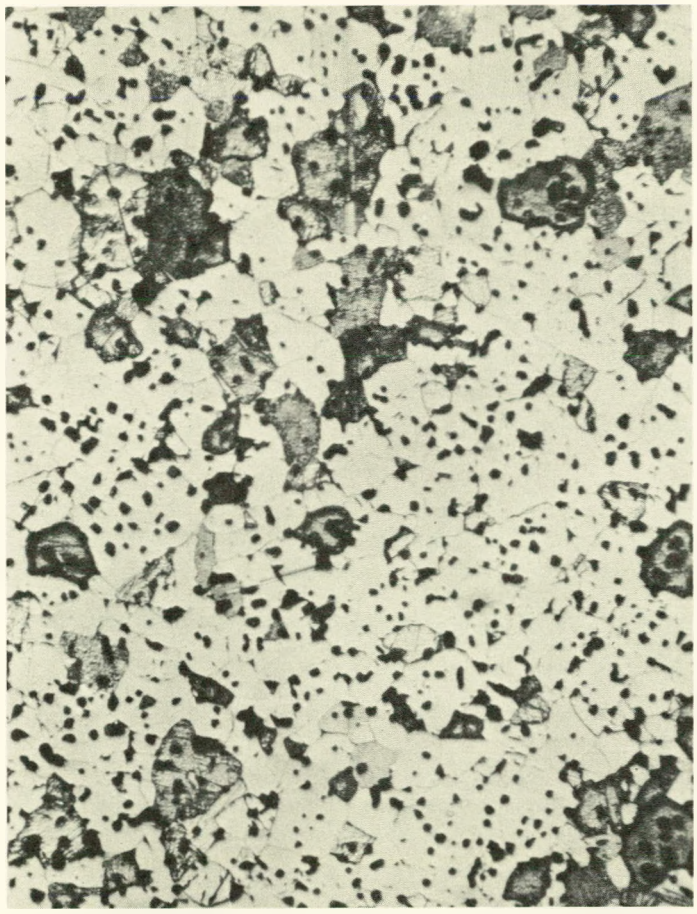

100x

Figure 1. Photomicrograph of an ETI Sample, Polished and Etched, after 2000°C Preliminary Anneal. (Small black areas are pores, large darkened areas are etched grains.)

was machined from the cylindrical sides after the diffusion anneal had been performed. The sample was then mounted with castable plastic within a cylindrical tube, as shown in Figure 2. For the first few samples this cylinder was aluminum; but since it appeared that thermal expansion of the aluminum could cause dimensional errors with small temperature changes, shorter cylinders of alumina, which has a smaller coefficient of thermal expansion, were used for subsequent mountings. The entire assembly was then ground down in minute steps on SiC abrasive paper and measured with a micrometer. Measurements were made both on the edges of the cylinder mount to ascertain removal of sample surface in parallel planes, and on the center of the exposed sample face to determine the amount of sample removed. Measurements were made to 2.5μ (0.0001 inch), and in most cases are probably accurate to $\pm 2.5\mu$.

So as to count the activity remaining in the sample at each stage of grinding, the sample was placed in a geometrically reproducible position under a scintillation detector probe within a massive lead shield. Measurements of background and a control sample of Be^7 were interspersed with the sample measurements, to allow for the proper data corrections. To obtain suitable statistics, 10,000 counts for each sample activity determination and 100,000 counts on each determination of Be^7 control sample activity were taken.

Certain experimental difficulties were encountered. First, surface roughness, slight tipping of the sample in the mount, and "crowning" — development of a spherical rather than a truly planar surface on the sample during grinding — caused slight errors. These, however, were taken into account for each sample as necessary, and the remaining uncertainty was incorporated into the final probable error figures. Second, some contamination by molybdenum vapor occurred with several samples. This contamination will be discussed in Section IV.

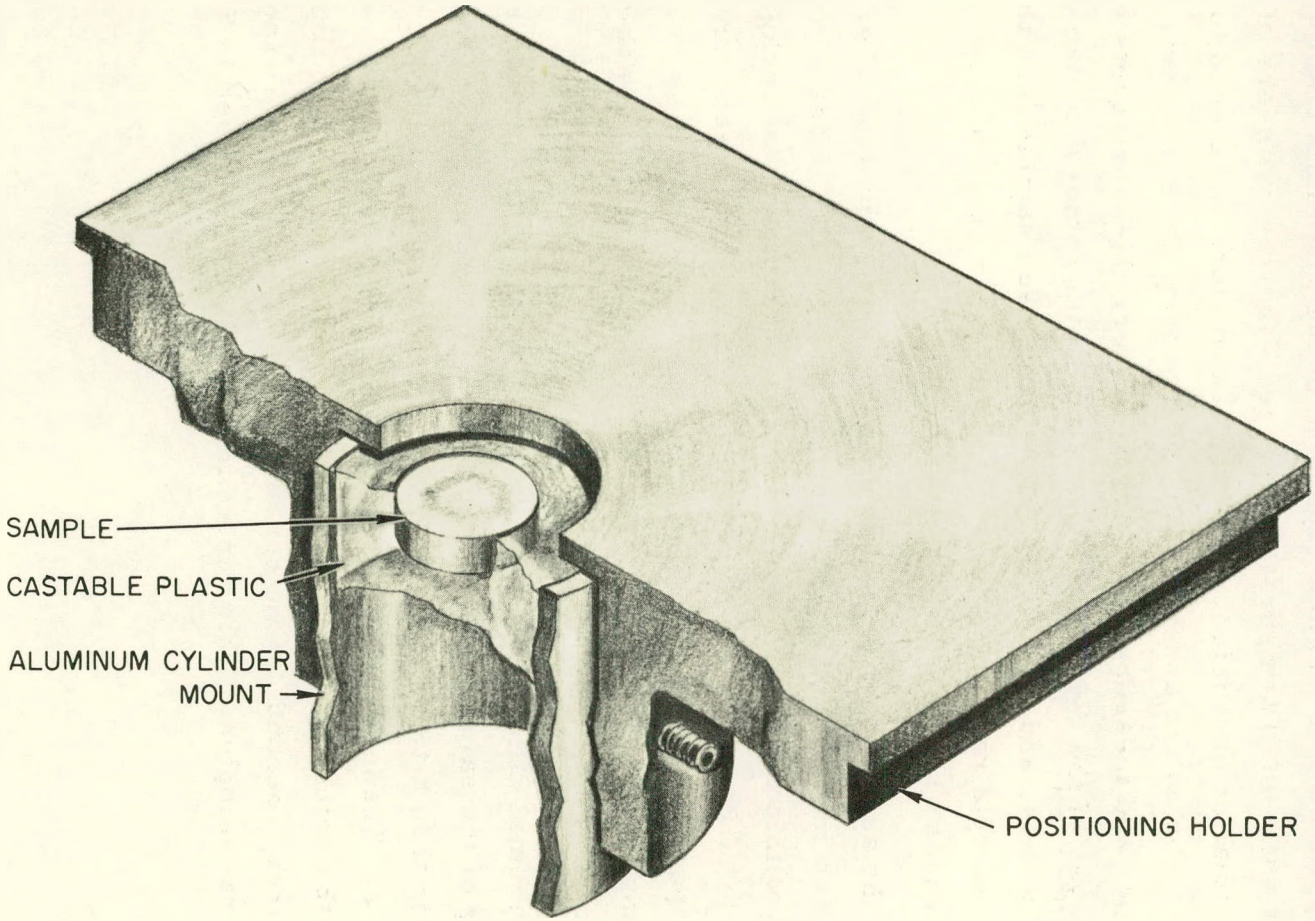

Figure 2. Cut-away Section of Plastic Mount and Holder for Positioning Sample Under Scintillation Counter

III. DATA AND ANALYSIS

The diffusion geometry used in this experiment was one-dimensional with a finite plane source. The solution[7] to the diffusion equation

$$\frac{\partial c}{\partial t} = D \frac{\partial^2 c}{\partial x^2} \qquad \ldots(1)$$

for this geometry is

$$C = \frac{N}{\sqrt{\pi Dt}} \exp\left(-\frac{x^2}{4Dt}\right) \qquad \ldots(2)$$

where

C = concentration

N = total amount of diffusing material, placed initially at x = 0

x = depth into sample in diffusion direction

t = time

and D = diffusion coefficient.

The experimental method does not directly measure the concentration C, but rather measures the integrated concentration for all depths below the ground surface. Therefore, we can define this measured quantity B as

$$B = \int_{x_o}^{\infty} c \, dx \qquad \ldots(3)$$

where x_o is the depth of sectioning. Note that for $x_o = 0$, B = N.

Equation (3) can be rewritten as

$$\frac{B}{N} = \frac{1}{(\pi Dt)}1/2 \int_{x_o}^{\infty} \left[\exp\left(-\frac{x^2}{4Dt}\right)\right] dx \qquad \ldots(4)$$

Now let $z = \frac{x}{2\sqrt{Dt}}$. Equation (4) then becomes

$$\frac{B}{N} = \frac{2}{\sqrt{\pi}} \int_{z_o}^{\infty} e^{-z^2} dz \qquad \ldots(5)$$

The right-hand member of equation (5) is, by definition,[7] the complementary error function for which tables and probability graphs have been constructed.[7] Consequently the data have been plotted on probability graph paper and analyzed according to equation (5).

The raw counting data have been corrected by subtracting background count; then normalized relative to the control sample. This normalization provides an automatic correction for radioactive decay as well as for long-term variations in instrumental efficiency. This normalized value is used to calculate B/N as used in equations (4) and (5).

In this normalized form, the data were plotted on probability graphs in Figures 3 through 9. If the diffusion process obeys equations 1 and 2, then B/N plotted vs x should yield a straight line. It is evident that straight lines can be drawn through the points, except for some points near x = 0. It was mentioned earlier that dimensional errors due to surface roughness, slight tipping, and errors in locating the original diffusion face, as for sample ET1-7, could be corrected. This is done by passing a straight line through the bulk of the points on a particular graph. The intersection of this straight line with B/N = 1.00 was considered to be the effective "zero" for depth dimensions, and was so included in the calculation. Since this is the case, the origin of the depth scale was arbitrarily chosen

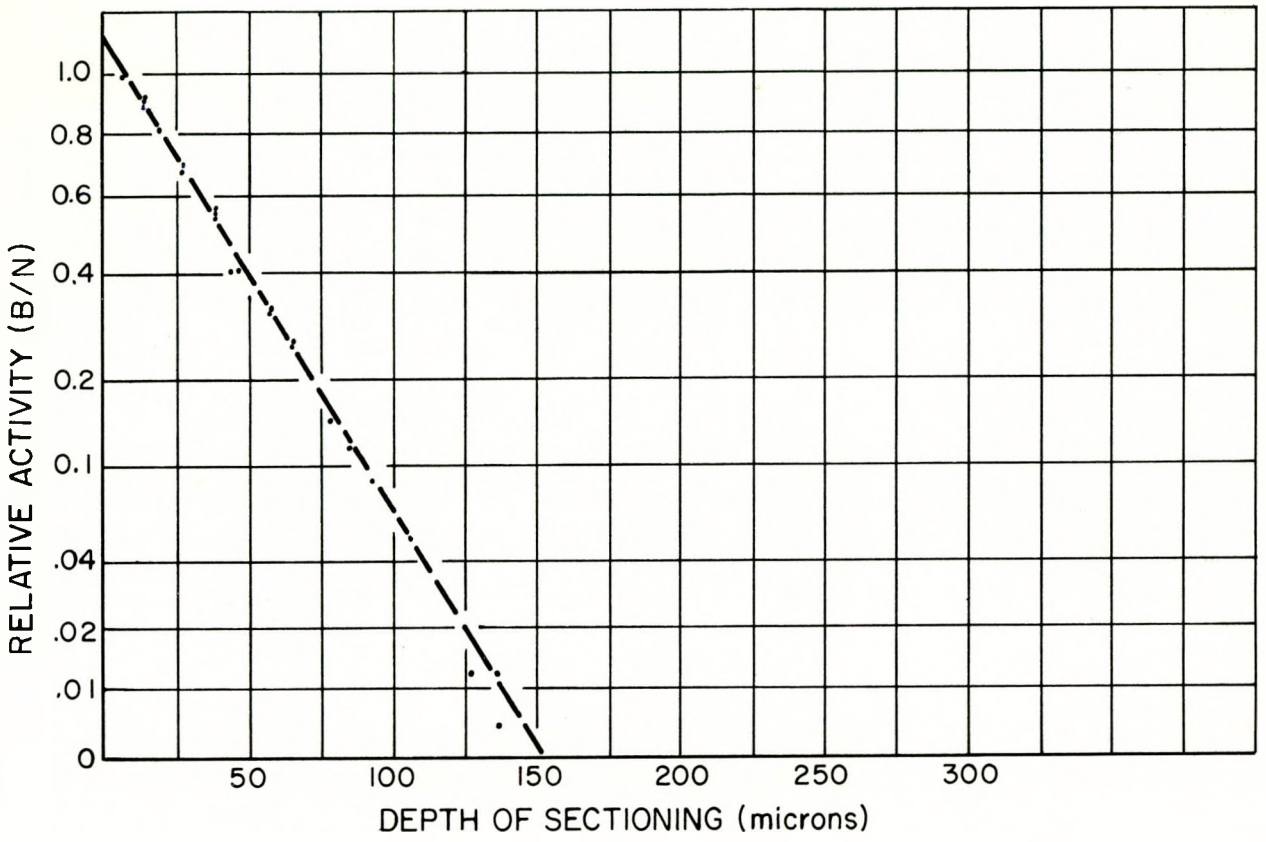

Figure 3. Be^7 Distribution after 1570°C Anneal

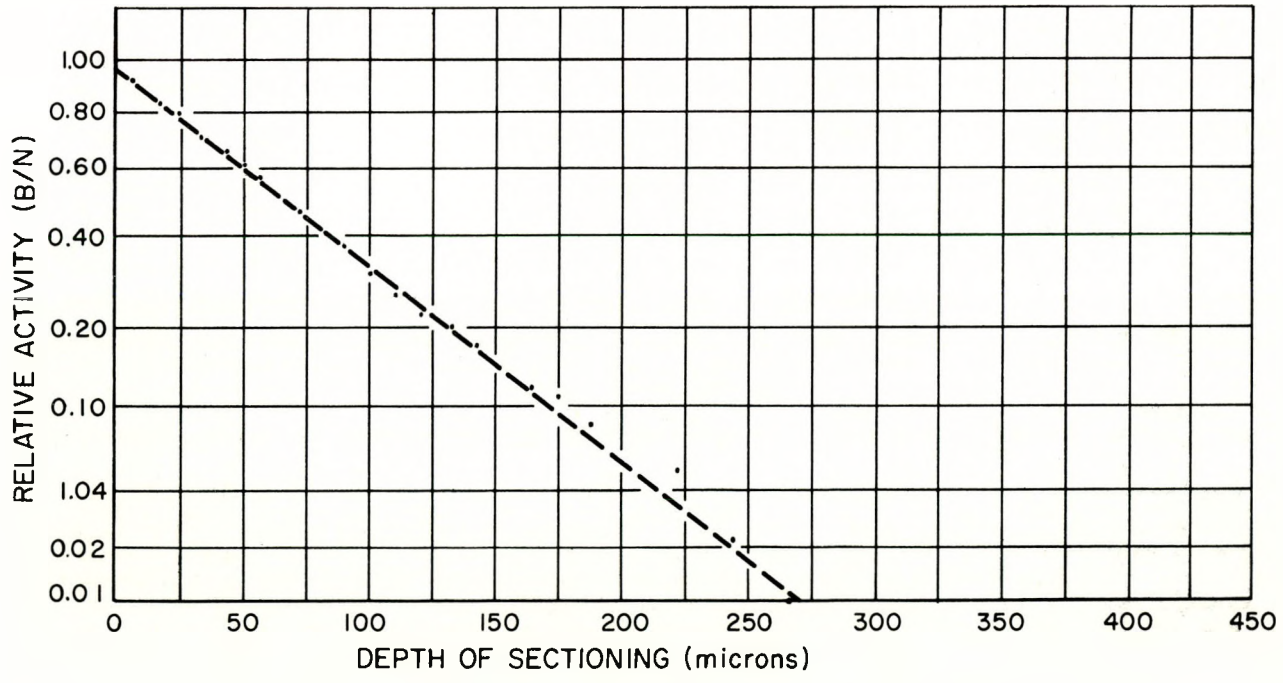

Figure 4. Be^7 Distribution after 1676°C Anneal

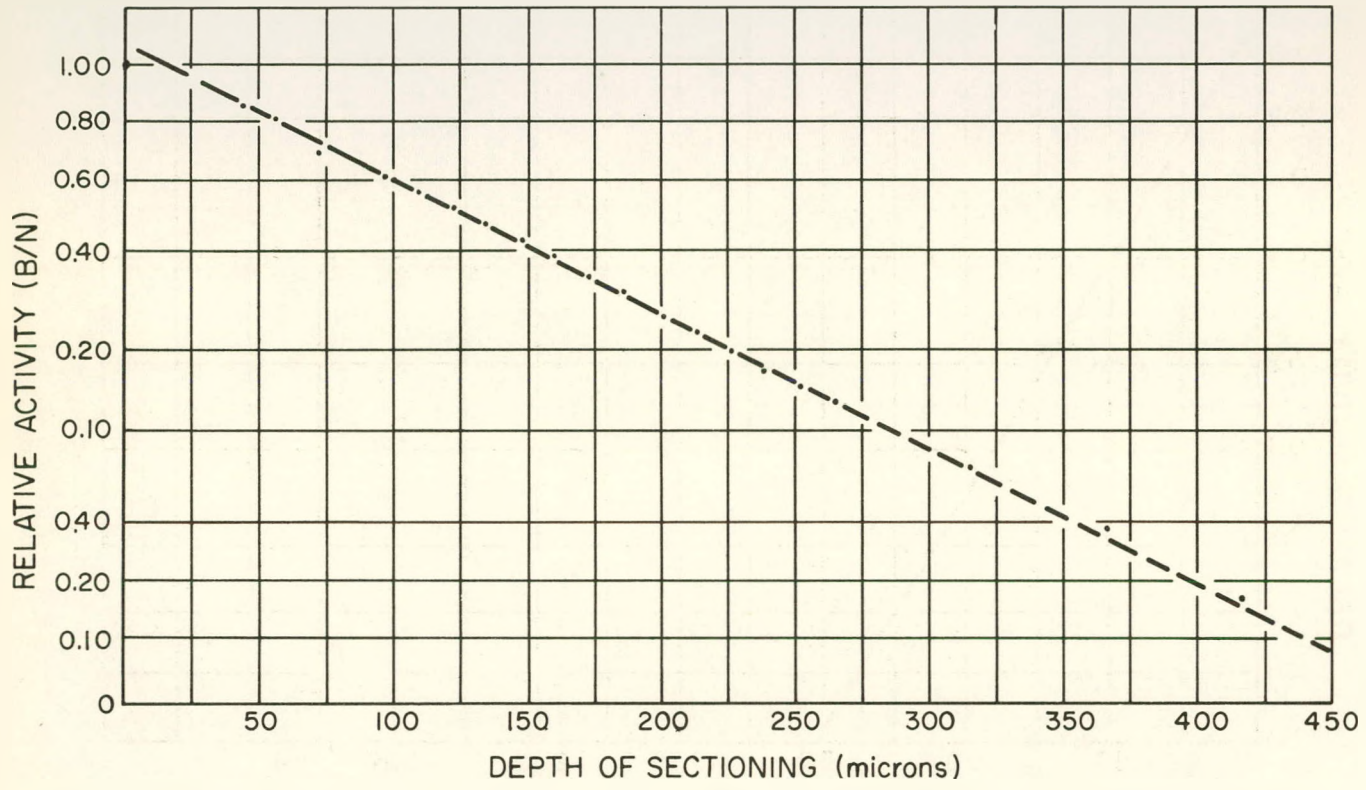

Figure 5. Be^7 Distribution after 1723°C Anneal

Figure 6. Be^7 Distribution after 1777°C Anneal

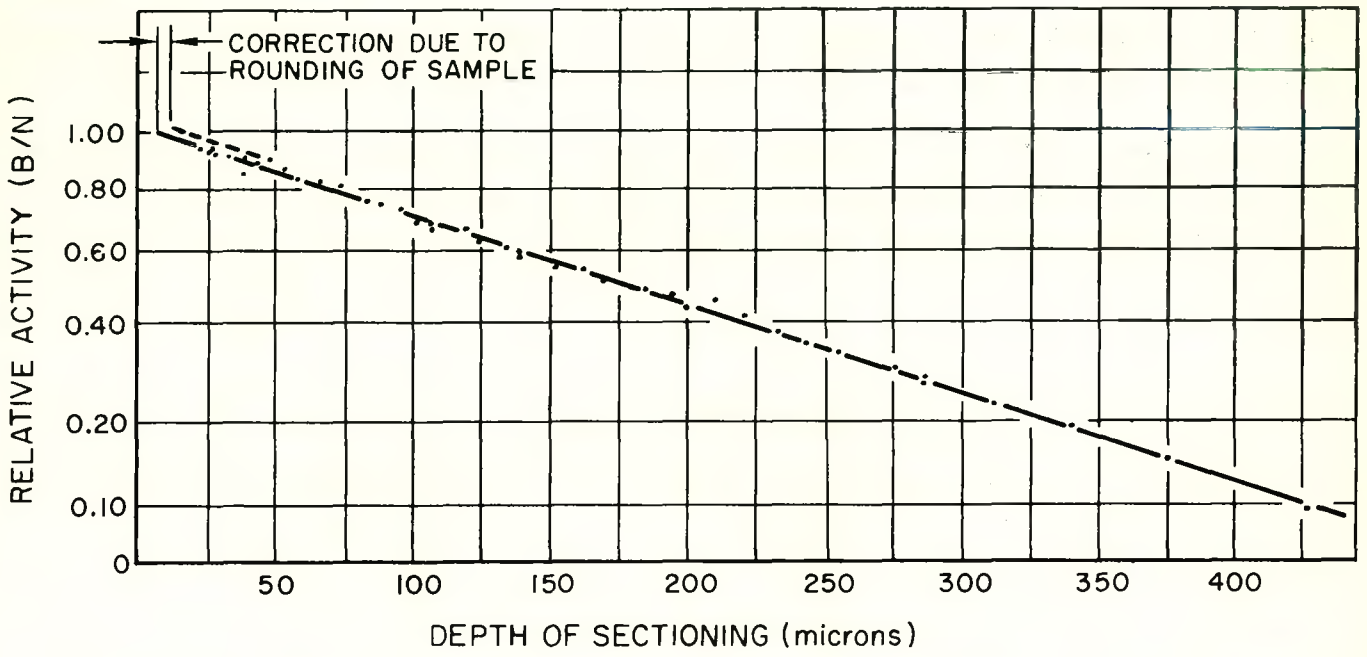

Figure 7. Be^7 Distribution after 1824°C Anneal

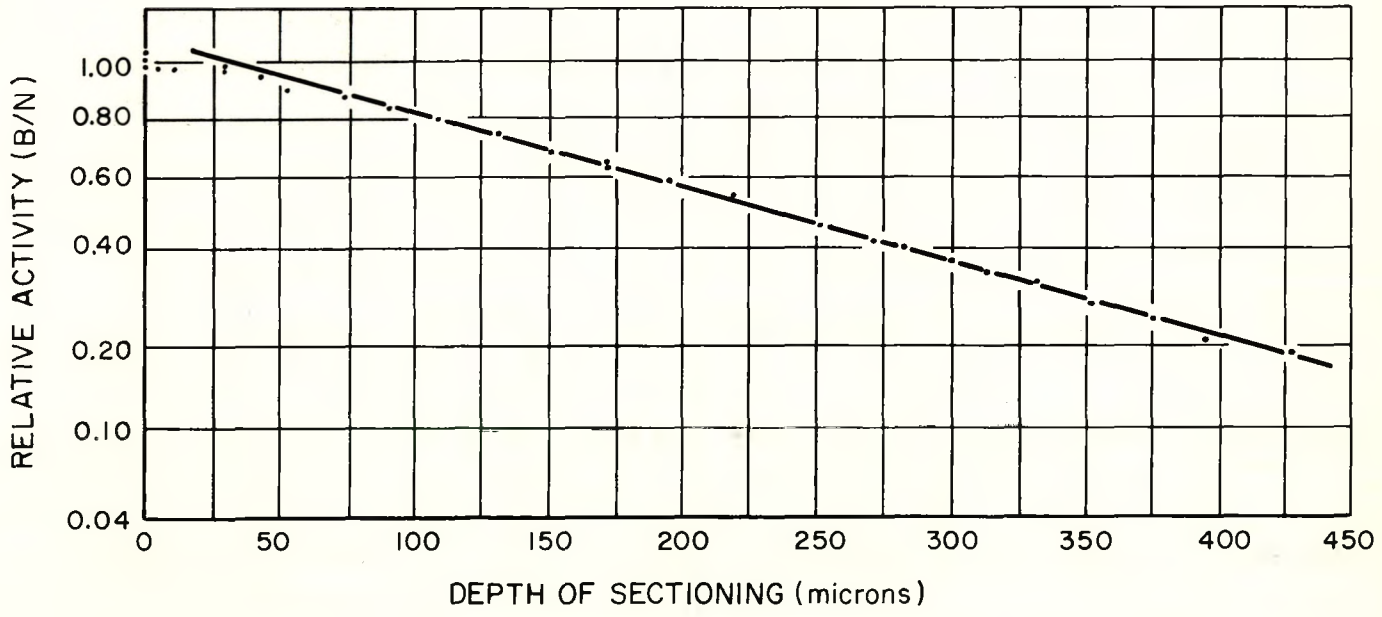

Figure 8. Be^7 Distribution after 1878°C Anneal

for convenience in several instances. The slight deviations near the intersection point can be attributed to the effect of surface roughness, or to slight tipping in the cases in which it was observed.

The values of diffusion temperature, time, and the corresponding diffusion coefficient D, as calculated from the data in Figures 3 to 9, are summarized in Table II, in the chronological order of analysis.

TABLE II

DIFFUSION DATA

Sample	Diffusion Anneal Temperature (°C)	Diffusion Anneal Time (sec)	D (cm^2/sec)	Remarks
ET1-11	1777 ± 10	3.64×10^4	5.35×10^{-9} ± 10%	Depth zero-point uncertain
ET1-4	1570 ± 10	3.63×10^4	3.43×10^{-10} ± 10%	Discoloration due to light contamination
ET1-7	1878 ± 10	3.66×10^4	1.19×10^{-8} ± 6%	Depth zero-point uncertain; discoloration due to light contamination
ET1-6	1676 ± 10	3.60×10^4	1.59×10^{-9} ± 11%	Discoloration due to heavy contamination
ET1-12	1934 ± 10	3.60×10^4	1.73×10^{-8} ± 3.4%	–
ET1-2	1824 ± 10	3.60×10^4	8.32×10^{-9} ± 7.4%	Correction required for "crowning"
ET1-5	1723 ± 15	3.61×10^4	3.67×10^{-9} ± 9%	–

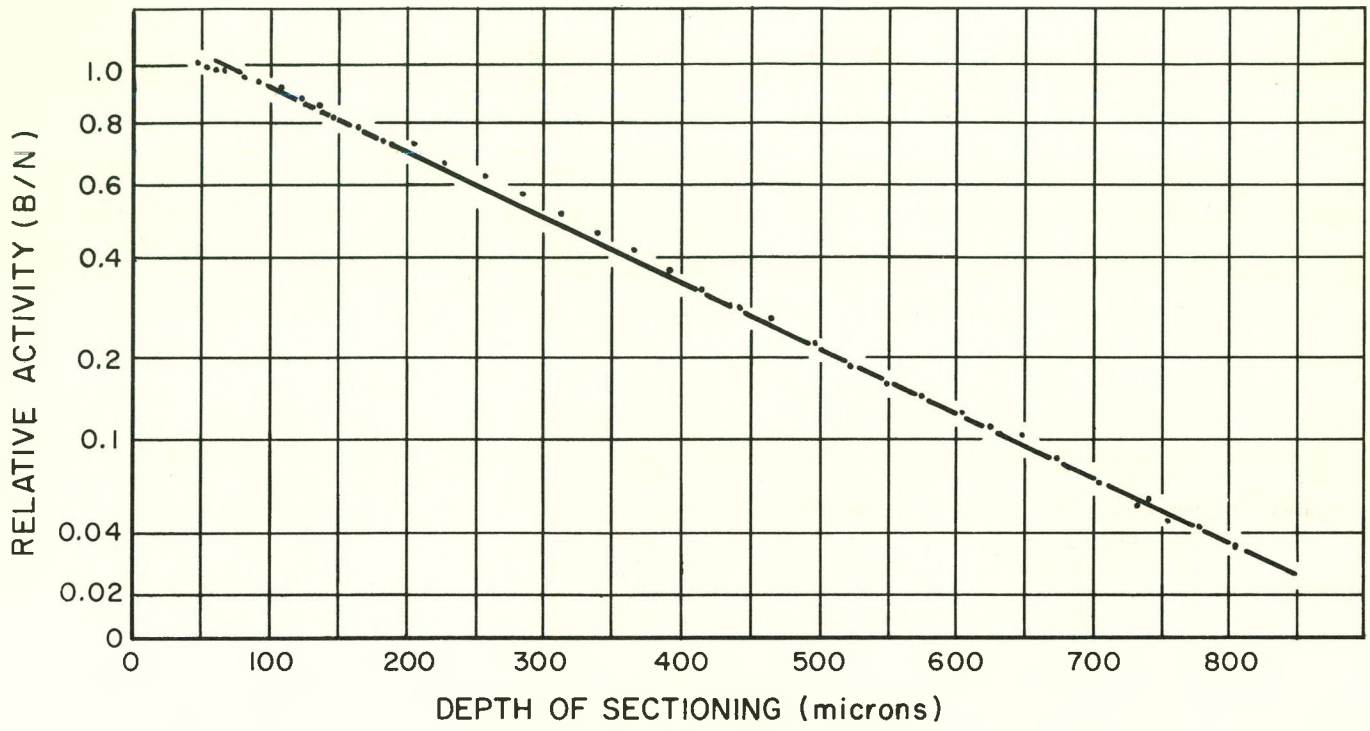

Figure 9. Be^7 Distribution after 1934°C Anneal

The data in Table II are plotted in Figure 10 as log D vs 1/T. From such a plot, the diffusion constant D_o and the activation energy can be evaluated for the customary equation

$$D = D_o \exp(-E/RT) \qquad \ldots(6)$$

where R is the molar gas constant, and E is the diffusion activation energy.

In Figure 10 it is evident that two regions can be represented by straight lines. These yield, for the low temperature region(1570° - 1730°C)

$$D = 5.56 \times 10^3 \exp\left[(-111{,}600 \pm 10{,}000)/RT\right] \qquad \ldots(7)$$

and for the high-temperature region (1730° - 1934°C)

$$D = 6.14 \times 10^{-2} \exp\left[(-66{,}100 \pm 2{,}000)/RT\right] \qquad \ldots(8)$$

IV. DISCUSSION

A. ALTERNATE DIFFUSION PROCESSES

In analyzing the experimental data, it was assumed that diffusion through the volume of the grains was the dominant process observed. However, competing processes of grain-boundary and surface diffusion have been observed in metals. Such phenomena are governed by lower activation energies and, when observed, are dominant at lower annealing temperatures than is the case for volume diffusion. These effects must therefore also be considered as possible in beryllia. After consideration, and for the following two reasons, it does not appear that grain-boundary or surface diffusion can account for the data presented here.

1) The effect of any possible surface diffusion is excluded from the analysis by prior removal of the cylindrical sides of the sample.

2) The possibility of grain-boundary diffusion was checked analytically. Fisher[8] and Smoluchowski[9] have both arrived at the conclusion that for grain-boundary diffusion, the logarithm of concentration should vary as $-x$, whereas for volume diffusion it should vary as $-x^2$. Since the present data fit the $-x^2$ relation* reasonably well, grain-boundary diffusion appears ruled out as a significant factor.

B. EFFECT OF MOLYBDENUM IMPURITY

The samples used in this experiment are believed to be identical in impurity content, except as Table II indicates, for molybdenum contamination. Several of the samples were discolored by Mo vapor from the muffle in which they were heated. Another sample, ETI-6, was accidentally contaminated to a relatively higher level. Microscopic examination showed this Mo to be distributed along grain boundaries: the atomic size of Mo probably excludes any significant extent of solid solution in BeO.

In Figure 10 are shown the points for 1723°, 1676°, and 1570°C; representing no contamination, relatively heavy contamination, and light contamination,

*Note that a linear plot on a probability graph is equivalent to a linear relation between log C and $-x^2$, as can be seen from equation (2).

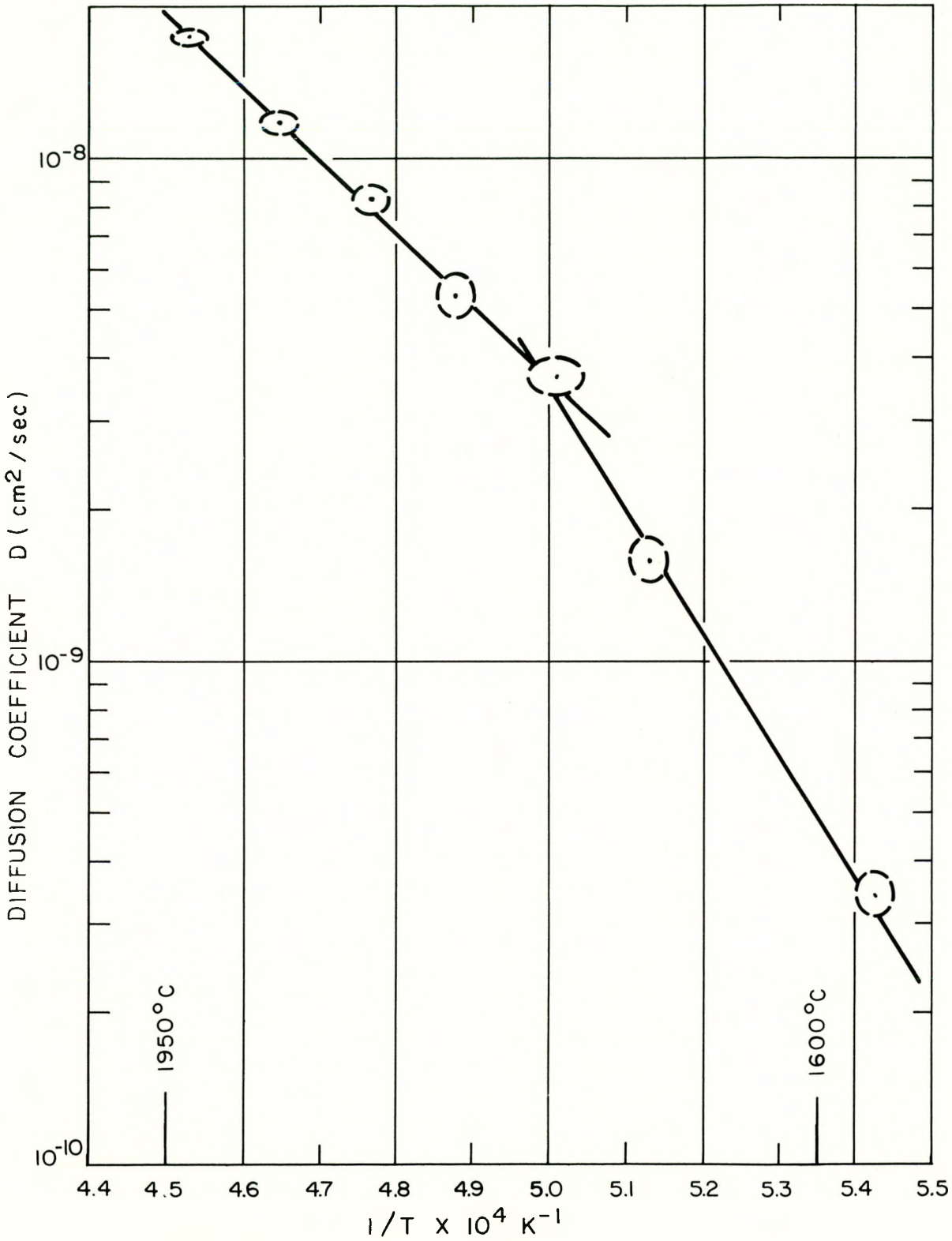

Figure 10. Log D vs 1/T for Diffusion of Be^7 in BeO

respectively. The distribution of these points along the straight line drawn shows that although possibly Mo can reduce the diffusion rate slightly, the extent of such an effect, if any, does not exceed the experimental error. The distribution also shows that the presence of Mo in the samples cannot possibly account for the break in the log D vs 1/T curve.

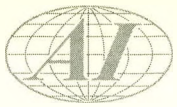

V. SUMMARY

Evaluation of Be^7 diffusion in BeO, by tracer methods, yielded values ranging from 3.43×10^{-10} cm^2/sec at 1570°C to 1.73×10^{-8} cm^2/sec at 1934°C, attributable to volume diffusion. The data show two regions of temperature-dependent diffusion. These regions are controlled by activation energies of 111,600 calories/mole between 1570° and 1730°C, and by 66,100 calories/mole between 1730° and 1934°C. It seems that different but possibly related mechanisms may account for the character of these two regions. Theoretical development of possible mechanisms will be presented in future reports.

The number of points obtained and shown in Figure 10 is not sufficient to establish a high level of confidence nor small probable errors in evaluation of activation energies. It is therefore unfortunate that there were not more samples of this identical material with which to obtain more points. Further, it is not yet known to what extent impurities, microstructure, or other material characteristics might affect the diffusion rate. Consequently the present data cannot be applied directly to other BeO materials with confidence until the mechanism of self-diffusion and the effects of material variables are known. In spite of this, the present data show a certain pattern of temperature dependence for this particular series of identical samples, and permit the importance of Be self-diffusion in BeO, as regards various material transport phenomena, to be estimated.

REFERENCES

1. T. J. Gray, "Defect Solid State," Interscience Publishers, 1957.

2. R. F. Walker, "Mechanism of Material Transport during Sintering," J. Am. Ceram. Soc. 38, (6) p. 187-97 (1955).

3. C. Herring, "Diffusional Viscosity of a Polycrystalline Solid," J. Appl. Physics, 21, p. 437 (1950).

4. J. M. Hollander, I. Perlman, and G. T. Seaborg, "Table of Isotopes," Rev. Mod. Phys. 25, p. 476-613, (1953).

5. Nuclear data, NBS Circular 499, September 1, 1950.

6. S. B. Austerman, G. M. Wolten, and C. T. Broman, "A High-Temperature Vacuum Quench Furnace," NAA-SR-2312 (1958).

7. J. Crank, The Mathematics of Diffusion, Clarenden Press, Oxford, (1956).

8. J. C. Fisher, J. Appl. Physics, 22, p. 74-77 (1951).

9. R. Smoluchowski, "Theory of Grain Boundary Diffusion," Phys. Rev. 87, p. 482-87 (1952).